Food and Chemical Toxicology 212 (2026) 116062

Contents lists available at ScienceDirect

Food and Chemical Toxicology

journal homepage: www.elsevier.com/locate/foodchemtox

Paternal exposure to low-dose N-nitrosodimethylamine (NDMA) induces intergenerational alterations in the prostatic microenvironment of rats

Karen Gabriela Favaro de Souza [a,b], Gabrielle Chalupa Faria [a,b], Débora Hipólito Quadreli [a,b], Ivana Regina da Costa [a,b], Bárbara Campos Jorge [c], Lívia Trippe Nagaoka [c], Julia Stein [c], Vanessa Aguiar Rocha [c], Arielle Cristina Arena [c], Wellerson Rodrigo Scarano [c], Glaura Scantamburlo Alves Fernandes [a,*]

[a] Department of General Biology, Center for Biological Sciences, State University of Londrina - UEL, Londrina, Paraná, Brazil
[b] Department of Immunology, Parasitology and General Pathology, Center for Biological Sciences, State University of Londrina - UEL, Londrina, Paraná, Brazil
[c] Department of Structural and Functional Biology, São Paulo State University "Júlio de Mesquita Filho" - UNESP, Botucatu, São Paulo, Brazil

ARTICLE INFO

Handling Editor: Professor Matthew Wright

Keywords:
NDMA
Environmental contaminant
Toxicity
Prostate
POHaD

ABSTRACT

NDMA is a nitrosamine recognized as an environmental contaminant of water and food, unintentionally formed during industrial processes and water treatment. Due to its mobility in aquatic environments, persistence, and carcinogenic potential, NDMA has emerged as a toxicological and public health concern. This study evaluated the effects of low-dose exposure (7.2 ng/kg/day) on the prostate of male Wistar rats across two generations within the Paternal Origins of Health and Disease (POHaD) framework. F0 males were exposed via gavage from postnatal day (PND) 60 to 104. In F1, offspring were evaluated at PND70 (paternal exposure) and PND120 (direct exposure PND22-70). Exposed F0 males showed increased prostate weight. Stereology revealed epithelial expansion and luminal reduction in F0 and F1 (PND120), increased interstitial area in paternally exposed offspring, and reduced interstitium in F1 (PND70). Collagen analyses showed reduced type III in F0 and reduced types I and III in F1 (PND70), while type I increased in F1 (PND120) with exposure. All groups exhibited inflammatory infiltrate and mast cell degranulation. RT-qPCR indicated decreased androgen receptor (Ar) expression in F1 (PND120) with exposure, reduced Tnf-α in exposed F1, and increased Il-6 only in exposure. NDMA induced direct and intergenerational prostatic toxicity, reinforcing the POHaD concept.

1. Introduction

Humans and other animals are constantly exposed to environmental pollutants through various sources such as contaminated water and food, inhalation of polluted air, or skin contact (Nash et al., 2004). N-nitrosodimethylamine (NDMA) is a nitrosamine widely present in different sources of contamination, known for its mutagenic and carcinogenic potential (Beard and Swager, 2021). It can be unintentionally generated in industrial processes that use nitrite/nitrate and amines (US-EPA, 2016). In the environment, it is present in drinking water and smoked and grilled food, dairy products, and vegetables (Anvisa, 2021).

Exposure to toxic substances can cause epigenetic alterations in germ cells, which are passed on to subsequent generations (Skinner and Anway, 2005), especially exposure during critical developmental periods, such as during gametogenesis or in early stages of life (Roth and Sweatt, 2011; Guerrero-Bosagna and Skinner, 2009). During this postnatal phase, the maturation of the hypothalamic-pituitary-gonadal axis occurs (Golub et al., 2008). Therefore, these developmental periods are more susceptible to toxic substances, which can cause immediate or permanent damage to the reproductive system, and it is widely recognized that several environmental pollutants can impact male reproductive health (Chen et al., 2017; Erthal et al., 2017).

The prostate is the main accessory gland of the male reproductive system, contributing to the production of nutrients during ejaculation (Kumar and Majumder, 1995) and playing a fundamental role in semen liquefaction and sperm capacitation, assisting the reproductive process (Kalinska et al., 2016). Its physiology is entirely dependent on androgens, which, upon binding on the androgen receptor (AR), regulate the synthesis of essential proteins for the proliferation and secretion of prostatic epithelial cells (Wilson, 2011). In rodents, the prostate has

* Corresponding author.
E-mail address: glaura@uel.br (G.S. Alves Fernandes).

https://doi.org/10.1016/j.fct.2026.116062
Received 15 December 2025; Received in revised form 9 March 2026; Accepted 10 March 2026
Available online 11 March 2026

three lobes: ventral, dorsolateral, and anterior (Sugimura et al., 1986). The ventral prostate was selected due to its high sensitivity to hormonal and environmental changes, being the most androgen-responsive lobe and, therefore, the most commonly used in studies on prostatic lesions, as well as in toxicological and developmental research. (Scarano et al., 2009).

There is a growing acknowledgement of the importance of studying the role of parents in their children's health, aligned with the concept of Paternal Origins of Health and Disease (POHaD) (Dolinoy; Jirtle, 2008). Genomic contributions, such as DNA alterations, and epigenomic contributions, such as modifications in sperm DNA methylation, can be influenced by environmental exposures, paternal age and nutrition, impacting the fertility and health of offspring (Soubry et al., 2014). Thus, certain stimuli before conception can affect the future health of the progeny through epigenetic programming in germ cells (Khoshkerdar et al., 2021). Evidence indicates that exposure to NDMA is associated with an increased risk of prostatic cancer development (Lee and Cho, 2024). Studies from our group showed that combined maternal and paternal exposure of Wistar rats to NDMA (7.2 ng/kg/day), from PND 60 to PND 90 and extended throughout gestation (GD 0 to GD 20), induced alterations in maternal hematological parameters and specific effects on fetal development, notably an increased number of fetuses larger than expected for gestational age fetuses and a higher incidence of supernumerary ribs (Alves et al., 2025).

Therefore, the goal of this study was to evaluate the effects of low-dose NDMA exposure on the prostate of Wistar rats from the F0 and F1 generations, investigating both paternal exposure effects and direct exposure in the offspring, in order to understand intergenerational impacts within the concept of Paternal Origins of Health and Disease (POHaD).

2. Materials and methods

2.1. Animals

A total of 40 male and 40 female Wistar rats (n = 10/group/sex) were obtained from the Central Vivarium of UNESP. The animals arrived at the facility at 35 days of age and underwent a 25-day acclimation period under controlled environmental conditions (22 °C, 12 h light/12 h dark cycle, relative humidity ~50%), with free access to water and commercial feed. After acclimation, at 60 days of age, males and females weighed approximately 200 g and 150 g, respectively, and were allocated to the experimental groups and subjected to the exposure protocol. Experimental procedures were conducted in accordance with the Ethical Principles of the National Council for the Control of Animal Experimentation (CONCEA), complied with the Guide for the Care and Use of Laboratory Animals (NIH, USA), and followed the ARRIVE guidelines. All procedures were approved by the Ethics Committee on Animal Use (CEUA) of the Botucatu Institute of Biosciences, UNESP (protocol: 4704260423).

2.2. Chemical compound and dosage determination

N-nitrosodimethylamine (NDMA) was commercially acquired (NDMA; CAS 62-75-9; Sigma-Aldrich®, Cat. No. PHR2407; Lot LRAC8369; purity 97.3%). The selected dose was based on the acceptable daily intake (ADI) for humans of 96 ng/day (Anvisa, 2021; FDA, 2020), or approximately 2 ng/kg/day, and converted to the animal dose using the following formula: Human Dose = Animal Dose x (Animal Weight/Human Weight) ^0.25 (US EPA, 2014). Thus, considering an average human weight of 50 kg, average animal weight of 0.30 kg, and a human dose of 2 ng/kg/day, a dose of 7.18 ng/kg/day, approximately 7.2 ng/kg/day of NDMA, was obtained. Exposure was performed orally, via gavage. NDMA was diluted in deionized water and administered orally at a dose of 7.2 ng/kg/day. The administered volume was adjusted according to the body weight of each animal, using deionized water as the solvent/vehicle in the NDMA group. The control group received the same volume of deionized water. Although this approach is commonly applied in toxicological risk assessment, it relies on assumptions of proportional metabolic and pharmacokinetic relationships between species. Therefore, direct equivalence between rat and human exposure cannot be assumed, particularly regarding NDMA biotransformation and tissue susceptibility.

2.3. Experimental design

2.3.1. Generation F0

The experimental design is summarized in Fig. 1. Males of the F0 generation were continuously exposed from PND60 to PND104, a period that encompasses approximately one complete spermatogenic cycle in rats (Russell et al., 1990). Mating occurred between PND90 and PND104, therefore, the spermatozoa used for fertilization developed during NDMA exposure.

After the paternal pre-conception exposure period, one male rat was paired with one female rat (1:1). For this, a vaginal lavage was performed on females to identify cells in estrus, and when identified, they were placed to mate during the dark cycle. Pregnancy confirmation was achieved through a new lavage for sperm detection. Therefore, if pregnancy was not confirmed, the animals continued in the second phase of exposure for up to 14 days (estimated period for the occurrence of 3 to 4 complete estrous cycles, or approximately 3 to 4 pregnancy attempts). Regardless of pregnancy confirmation, males remained under exposure until PND104 to standardize the exposure period.

The animals were divided into two experimental groups (n = 10 animals/group): 1) Control Males; 2) NDMA Males. Exposure was performed orally, via gavage. For control animals, 1 mL/kg of distilled water was administered, and for NDMA groups, 7.2 ng/kg/day of NDMA was administered, with a final administration volume of 1 mL/kg.

2.3.2. Generation F1

The offspring resulting from F0 matings were allocated for the continuation of this study (F1 generation). After birth, the litter was randomly reduced to 10 pups per litter (5 males and 5 females).

Part of the male pups were kept in the vivarium for exclusive evaluation of paternal exposure (F1 PND70 group; n = 1/litter). These animals were divided into 2 experimental groups according to paternal exposure (n = 10 per group): 1) Control Offspring (control males X control females); 2) Paternal NDMA Offspring (NDMA males X control females).

Another portion of male pups was designated for direct exposure (F1 PND120 group). This experimental branch was included to evaluate the effects of direct NDMA exposure in the offspring independently of paternal exposure. Exposure was performed via gavage from weaning (PND22) until the end of sexual maturation (PND70). Each litter consisted of 2 male pups that underwent this exposure, divided into a control group that received 1 mL/kg/day of distilled water and an exposed group that received 7.2 ng/kg/day of NDMA, with a final administration volume of 1 mL/kg.

The exposed F1 generation experimental groups were organized as follows:

- Control: Control father and offspring;
- FC: Exposed father and control offspring;
- CE: Control father and exposed offspring;
- FE: Exposed father and exposed offspring;

F0 males were euthanized at PND104. In the offspring, F1 generation males exclusively exposed paternally were euthanized at PND70, and those exposed during sexual maturation were euthanized at PND120. For this, animals were anesthetized with sodium thiopental, followed by cardiac puncture.

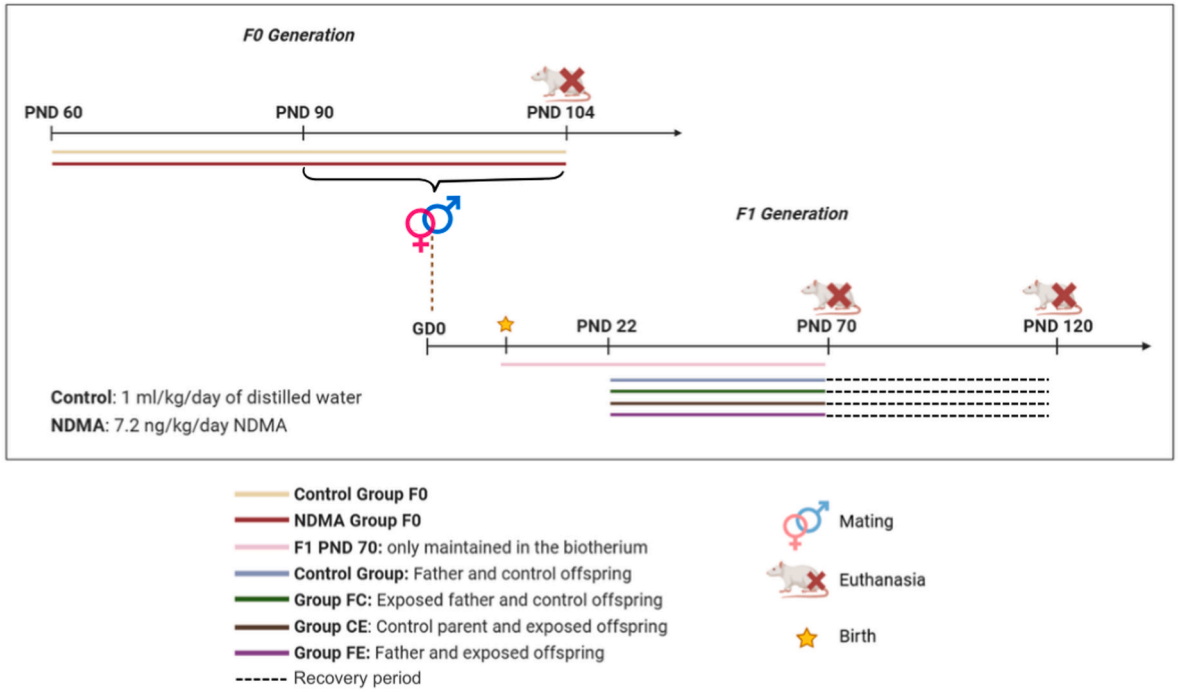

Fig. 1. Experimental design of this study. PND = postnatal day, GD = gestational day.

2.4. Sample processing

The prostate of each animal was collected, weighed, and divided into two parts: one half was used for histological analyses, while the other half was stored at −80 °C for oxidative stress and gene expression analyses.

The ventral prostate was removed and fixed in Methacarn (60% methanol, 30% acetic acid, and 10% glacial acetic acid) for 4 h. After the fixation period, it proceeded to the Paraplast® embedding process, where the material was immersed in baths (30 min each) of alcohol (95% and absolute), xylene (1 h), and Paraplast®. The last xylene and Paraplast® baths were performed in an oven at 65 °C. Subsequently, the material was sectioned into 5 μm slices and stained with hematoxylin and eosin (HE) for stereology and histopathology analyses, as well as with 1% toluidine blue for mast cell counting and Picrosirius for quantification and differentiation of type I and type III collagen.

2.5. Stereological analysis

Stereological evaluation of the prostate was performed using transverse sections of the organ with the aid of a microscope at 40x objectives. Images for photo documentation were captured by a microscope coupled to a digital camera and a microcomputer. Stereological analysis was conducted according to the method of Weibel (1963), which uses a test system of lines and points on a grid with 168 points and 60 lines. Thus, the proportion of the section occupied by the lumen, epithelium, and interstitium was obtained (Punhagui et al., 2016).

2.6. Histopathological analysis - qualitative evaluation

Histopathological evaluation of the prostate was conducted using transverse sections of the organ stained with hematoxylin and eosin and evaluated with the aid of a microscope equipped with 40x objectives. Images for photo documentation were captured by a microscope coupled with a digital camera and a microcomputer, obtaining ten photomicrographs of each segment. For histopathological analysis, qualitative aspects of the prostate epithelium and interstitium were examined, such as presence of inflammatory infiltrate and cells in the glandular lumen. Images were captured with each field covering an area of 0.03146 mm^2. The histopathological evaluation was initially performed by the principal investigator using predefined morphological criteria. All slides were subsequently reviewed by an independent observer, blinded to group allocation, to confirm the reproducibility of the results.

2.7. Histopathological analysis – semi-quantitative evaluation

Histopathological evaluation was performed on hematoxylin and eosin–stained sections of the ventral prostate. For each animal, five sections were analyzed, and ten fields (400 ×) per section were randomly selected for evaluation.

Lesions were assessed using predefined morphological criteria according to Gibson-Corley et al. (2013). Inflammatory infiltrate and the presence of inflammatory cells in the glandular lumen were evaluated using a four-level ordinal semi-quantitative scoring system based on the proportion of affected microscopic fields:

- Score 0 – No lesions observed
- Score 1 – Mild involvement (<25% of affected fields)
- Score 2 – Moderate involvement (25–50% of affected fields)
- Score 3 – Marked involvement (>50% of affected fields)

2.8. Mast cell count

Mast cell counting analysis was performed as described by Punhagui et al. (2016). Tissue sections were stained with 1% toluidine blue for mast cell identification. Considering that mast cell granules contain heparin and sulfated glycosaminoglycan, they were metachromatically stained using toluidine blue to evaluate and quantify intact and degranulated mast cells. Mast cells were classified by optical light microscopy for the presence of granulated or degranulated metachromatic granules in the surrounding connective tissue. Ten photomicrographs of each segment were obtained. In all analyzed fields, mast cells were classified as intact or degranulated. The total mast cell count was performed according to Mendes et al. (2011) with adaptation. The quantification of intact and degranulated mast cells as well as the total number of mast

cells found in the photomicrographs was counted for each animal. Images were randomly captured with each field covering an area of 0.03146 mm^2.

2.9. Quantification of type I and III collagen

Quantification of collagen type I and III was performed according to Bueno et al. (2024). Histological sections were stained with Picrosirius, and ten images of each animal were captured using a high-resolution AxioCam camera (Carl Zeiss, Germany), coupled to an Axioscop Plus microscope (Carl Zeiss, Germany; 40x objective) and AxioVisionRel 4 software. Picrosirius-stained slides were examined under polarized light, allowing the differentiation of collagen types based on the intensity of birefringent fibers. In this method, type I collagen fibers appear red, while type III collagen fibers appear green. Analysis was performed using the RGB tool of ImageJ software, which separates the red, green, and blue channels of RGB images (ImageJ, 2004), enabling the identification and quantification of collagen fibers. Subsequently, the Color Segmentation plugin of ImageJ was used to quantify the pixels corresponding to each collagen type, and the results were expressed as the percentage of pixels for each fibrillar component.

2.10. Assessment of the oxidative profile

The oxidative stress assessment included the quantification of lipid peroxidation, a process that indicates cell membrane damage due to lipid oxidation. In addition, other antioxidant substances were measured, such as antioxidant enzymes that play important roles in cellular defense against oxidative damage.

2.10.1. Lipid peroxidation

The concentration of thiobarbituric acid reactive substances (TBARS) was evaluated as described by Federici and collaborators (2007). The concentration of MDA, an intermediate product of lipid peroxidation, was determined from the difference in absorbances read at 535 and 572 nm (Multiskan GO; Thermo Scientific, Vantaa, Finland). Results were expressed in nmmol/mg of protein.

2.10.2. Glutathione S-transferase

Glutathione S-transferase activity was evaluated spectrophotometrically using GSH, 1-chloro-2,4-dinitrobenzene (CDNB), and potassium phosphate buffer. Sample absorbance was measured at 340 nm for 5 min at 40-s intervals, as described by Keen and collaborators (1976). Results were expressed in nmmol.min-1.ml-1.mg of protein-1.

2.10.3. Catalase (CAT)

Catalase enzymatic activity was determined by the degradation of hydrogen peroxide into oxygen and water. After protein concentration determination (normalized to 1.0 mg/ml in PBS), 297 μl of reaction medium was placed in a UV4 microplate (in duplicate) at 240 nm for 60 s (AEBI et al., 1984). Results were expressed in mM.min-1.mg of protein-1.

2.10.4. Superoxide dismutase (SOD)

Superoxide dismutase enzyme activity was evaluated according to Senthilkumar and collaborators (2021) with some modifications. The enzyme was derived from homogenates normalized to 1 mg/ml. A reactive mixture containing sodium carbonate buffer (50 mM, pH 10.2), nitroblue tetrazolium (NBT) (96 μM) and Triton X-100 (0.6%) was prepared, which was incubated for 2 min with hydroxylamine hydrochloride (NH2OH· HCl) (20 mM, pH 6.0). The final volume was adjusted to 200 μL. The reaction consists of quantifying complexes formed by superoxide anions with the addition of NBT and NH2OH· HCl of yellowish coloration with the reduction of NBT, forming a bluish coloration read at 560 nm for 2 min at 15-s intervals. Results were expressed in units of SOD activity, according to the formula proposed by Zhang and collaborators (2016). Results were expressed in U.min-1.mg protein-1.

2.10.5. Reduced glutathione (GSH) and total glutathione (GT)

Reduced glutathione (GSH) and total glutathione (GT) levels were determined according to the method proposed by Rahman et al. (2007) with some modifications, using 5,5′-dithiobis-2-nitrobenzoic acid (DTNB) in the homogenate, resulting in the formation of a yellow-colored complex.

For the determination of total glutathione (GT) levels, DTNB, nicotinamide adenine dinucleotide phosphate (NADPH), and glutathione reductase were added to the homogenate. Both GT and GSH levels were measured at 412 nm (Multiskan GO, Thermo Scientific, Vantaa, Finland), and results were expressed in μmol/mg of protein. Glutathione disulfide (GSSG) levels were calculated as described by Carrara et al. (2019), considering the reaction stoichiometry. Results were expressed in μg.mg protein-1.

2.11. Evaluation of gene expression by real-time polymerase chain reaction after reverse transcription (RT-qPCR)

After euthanasia, ventral prostate samples collected were kept at −80 °C until use. RNA extraction (n = 5 animals/group) was performed with the TriZol kit (Ambion, USA) according to the manufacturer's instructions. Quantification, integrity, and purity of the material were verified by spectrophotometry in a NanoVueTM Plus (GE HealthCare Life Sciences, United States). The reverse transcription (RT) reaction was performed using the iScript™ cDNA Synthesis Kit (Bio-Rad Laboratories, Inc, CA, USA), as specified by the manufacturer. The mixture was incubated under the following conditions: 25 °C for 5 min, 42 °C for 30 min followed by reverse transcriptase inactivation at 85 °C for 5 min. Primers for the analyzed genes were designed using Primer Express® software (Applied Biosystems, Foster City, CA, USA), from sequences published in GenBank (www.pubmed.com), and synthesized by Invitrogen Life Technologies (Carlsbad, CA, USA). The primer sequences used for RT-qPCR are listed in Table 1.

Thermocycling was performed on a QuantStudio (Life Technologies, USA) instrument, obeying the following conditions: GoTag Hot Start Polymerase activation 2 min at 95 °C followed by 40 cycles of 15 s at 95 °C and 1 min at 60 °C, finally, a dissociation curve in the range of 60-95 °C. Reactions for each gene were elaborated in duplicates; for each sample, an amplification chart showing an increase in fluorescent reporter dye (ΔRn) in each PCR cycle was plotted. From this chart, the cycle where the reaction crosses the detection threshold (cycle threshold - CT) was determined. Relative quantification of each gene was performed using the 2-ΔΔ CT method according to (Rocha et al., 2023). Values obtained for all samples were normalized by the ratio obtained between target genes and the endogenous gene.

Table 1
List of primers designated for RTq-PCR.

Accession number	Primer	Sequence (5′–3′)
NM_199267.2	*Nf-Kb* F	CATACGCTGACCCTAGCCTG
	Nf-Kb R	GGTCTGCCCTCCTGACTCTA
NM_031144.3	*Actb F*	CTGTGTGGATTGGTGGCTCT
	Actb R	AGCTCAGTAACAGTCCGCCT
NM_012589.2	*Il6* F	ACTTCACAAGTCGGAGGCTT
	Il6 R	GCCATTGCACAACTCTTTTCTC
NM_012502.2	*Ar* F	CATTTCCGGAGACGACACCA
	Ar R	AAAAGAGGTGCGGAAGGGAA
NM_012854.2	*Il10* F	TGCGACGCTGTCATCGATTT
	Il10 R	TGGCCTTGTAGACACCTTTGT
NM_012675.3	*Tnf F*	GGAGGGAGAACAGCAACTCC
	Tnf R	GCCAGTGTATGAGAGGGACG

F: forward primer; R: reverse primer.

2.12. Statistical analysis

Homogeneity of variances was evaluated by Bartlett's test, while normality of distribution was verified by Shapiro-Wilk test. In F0 and F1 PND 70 generation groups, Student's t-test was applied for comparison between two groups with normal distribution and homogeneous variances, while Mann-Whitney test was used for non-parametric distribution. For F1 PND 120 generation groups, one-way analysis of variance (ANOVA) was applied, followed by Dunnett's post hoc test, for variables with normal distribution and homogeneous variances, or Kruskal-Wallis test, followed by Dunn's post hoc test, for non-parametric data. Results were considered statistically significant when $p < 0.05$. Statistical analyses and graph construction were performed using GraphPad Prism software (version 9.3.0), GraphPad Software, La Jolla, California, USA.

3. Results

3.1. Prostate weight and stereology

The absolute and relative prostate weights (Table 2) differed between the control group and the NDMA group only in the F0 generation. In this group, a significant increase in both weights (absolute and relative) was observed in animals exposed to NDMA. In F1 generations (PND70 and PND120), there was no significant difference in absolute and relative prostate weights when compared to the control group.

Stereological analysis (Table 3) showed that F0 generation animals exposed to NDMA presented an increase in epithelial proportion and a decrease in luminal proportion when compared to the control group; interstitial stereology showed no significant alteration (see Table 4).

Stereology of the F1 PND70 generation showed that animals whose fathers were exposed to NDMA presented a significant decrease in the interstitial compartment; the other parameters showed no significant alterations. In contrast, the F1 PND120 generation showed that all experimental groups exposed to NDMA indirectly or directly presented an increase in the epithelial compartment and a decrease in the lumen; the interstitium presented a significant increase only in the group where the father was exposed to the toxic substance, but not the offspring (FC).

3.2. Quantification of collagen type I and III

Analysis of collagen quantification under polarized light (Fig. 2) showed that in the F0 generation there were no significant differences in the percentage of type I collagen in the NDMA group relative to control, while type III collagen decreased (Fig. 2D). In the F1 PND70 generation, there was a decrease in collagen type I and III relative to the control group (Fig. 2E). The F1 PND120 generation showed a significant increase in collagen type I only in the father and offspring exposed to NDMA (FE) group; the other parameters showed no significant difference in this generation (Fig. 2F).

Table 2
Absolute and relative weight of the prostate.

Groups	Absolute weight (mg)	Relative weight (mg/kg)
F0		
Control	441.1 ± 17.65	103.9 ± 4.80
NDMA	530.4 ± 28.18*	128.5 ± 6.88*
F1 PND 70		
Control	243.5 ± 20.10	80.35 ± 5.72
NDMA	283.0 ± 12.73	86.23 ± 3.77
F1 PND 120		
Control	440.5 ± 26.10	97.04 ± 5.54
FC	475.0 ± 28.00	104.8 ± 6.04
CE	492.6 ± 38.85	108.7 ± 7.68
FE	484.5 ± 54.92	103.9 ± 11.68

Values expressed as median ± S.E.M (n = 10 per group). Statistical analyses performed with T-test for F0 and F1 (PND 70) groups and One-way ANOVA test followed by Dunnett's test for F1 (PND 120) groups. Groups marked with * differ significantly from control ($p < 0.05$). FC, Exposed father and control offspring; CE, Control father and exposed offspring; FE, Exposed father and exposed offspring.

Table 3
Stereological analysis of prostatic tissue.

Groups	Epithelium (%)	Lumen (%)	Interstitium (%)
F0			
Control	17.86 (14.14-22.62)[a]	71.73 (66.07-78.57)[a]	8.63 (4.76-12.50)[a]
NDMA	28.27 (22.62-35.86)[b]	63.10 (54.76-70.83)[b]	8.33 (5.20-10.86)[a]
F1 PND 70			
Control	24.11 (16.07-31.25)[a]	60.12 (55.21-68.45)[a]	13.99 (9.97-18.01)[a]
NDMA	27.08 (21.88-33.93)[a]	63.69 (58.78-69.79)[a]	8.33 ± (5.35-11.31)[b]
F1 PND 120			
Control	13.69 (6.99-20.98)[a]	80.36 (65.48-88.24)[a]	5.95 (2.08-12.80)[a]
FC	24.11 (14.88-29.91)[b]	62.50 (51.64-74.40)[b]	12.50 (7.58-19.35)[b]
CE	23.51 (13.69-29.76)[b]	69.64 (57.14-79.17)[b]	8.33 (5.20-14.73)[a]
FE	19.64 (11.90-30.06)[b]	69.05 (55.51-81.70)[b]	8.92 (3.57-14.43)[a]

Values expressed as median (Q1-Q3) (n = 5 per group). Mann-Whitney statistical test for F0 and F1 (PND 70) groups and Kruskall-Wallis test with Dunn's post-test for F1 (PND 120) group. Different letters in the same column indicate statistically significant differences between groups compared only to the control group. PND, Postnatal day; FC, Exposed father and control offspring; CE, Control father and exposed offspring; FE, Exposed father and exposed offspring.

Table 4
Mast cell count.

Groups	Intact (mm^2)	Degranulated (mm^2)	Total (mm^2)
F0			
Control	26.60 ± 6.25[a]	5.00 ± 1.58[a]	31.60 ± 7.55[a]
NDMA	9.60 ± 2.58[b]	21.40 ± 4.23[b]	31.00 ± 5.65[a]
F1 PND 70			
Control	21.20 ± 2.92[a]	2.60 ± 1.03[a]	23.80 ± 1.96[a]
NDMA	6.60 ± 1.86[b]	9.00 ± 2.07[b]	15.60 ± 1.96[b]
F1 PND 120			
Control	25.40 ± 2.54[a]	7.40 ± 1.20[a]	32.80 ± 1.39[a]
FC	25.60 ± 4.04[a]	18.40 ± 1.56[b]	32.20 ± 4.84[a]
CE	17.60 ± 2.54[a]	22.00 ± 1.92[b]	39.60 ± 3.01[a]
FE	13.20 ± 2.22[b]	22.20 ± 2.39[b]	33.60 ± 2.31[a]

Values expressed as mean ± S.E.M. (n = 5 per group). Unpaired *t*-test. Different letters in the same column indicate statistically significant differences between the groups compared to the control group alone. PDN. Postnatal day; FC, exposed father and control offspring; CE, control father and exposed offspring; PE, father and exposed offspring. mean ± standard error (SEM).

3.3. Histopathology and mast cell count

Histopathological analysis of the F0 generation (Fig. 3A–C) showed the presence of inflammatory infiltrate in the prostatic tissue (Fig. 3 A) and cells in the lumen of the prostatic gland (Fig. 3 B) in the NDMA-exposed group. The exposed group also presented a decrease in intact mast cells (Fig. 4 A) and a significant increase in degranulated mast cells (Fig. 4 B) when compared to the control. There was no difference in the total number of mast cells in the prostate between the experimental groups (Fig. 4 C).

Histopathological analysis of the F1 PND 70 generation (Fig. 3D–F) showed no findings of inflammatory infiltrate or cells in the lumen. Mast cell count showed that the group indirectly exposed to NDMA also presented a decrease in intact mast cells (Fig. 4 D) and a significant increase in degranulated mast cells (Fig. 4 E). Additionally, the total number of mast cells in the prostate of the exposed group presented a significant decrease (Fig. 4 F).

Histopathological analysis of the F1 PND120 generation (Fig. 4G–R) showed the presence of inflammatory infiltrate in the prostate of all groups exposed indirectly and/or directly to NDMA (Fig. 3J–M, and P), as well as the presence of cells in the lumen (Fig. 3K–N, and Q). Only the group with paternal and direct exposure (PE) showed a decrease in

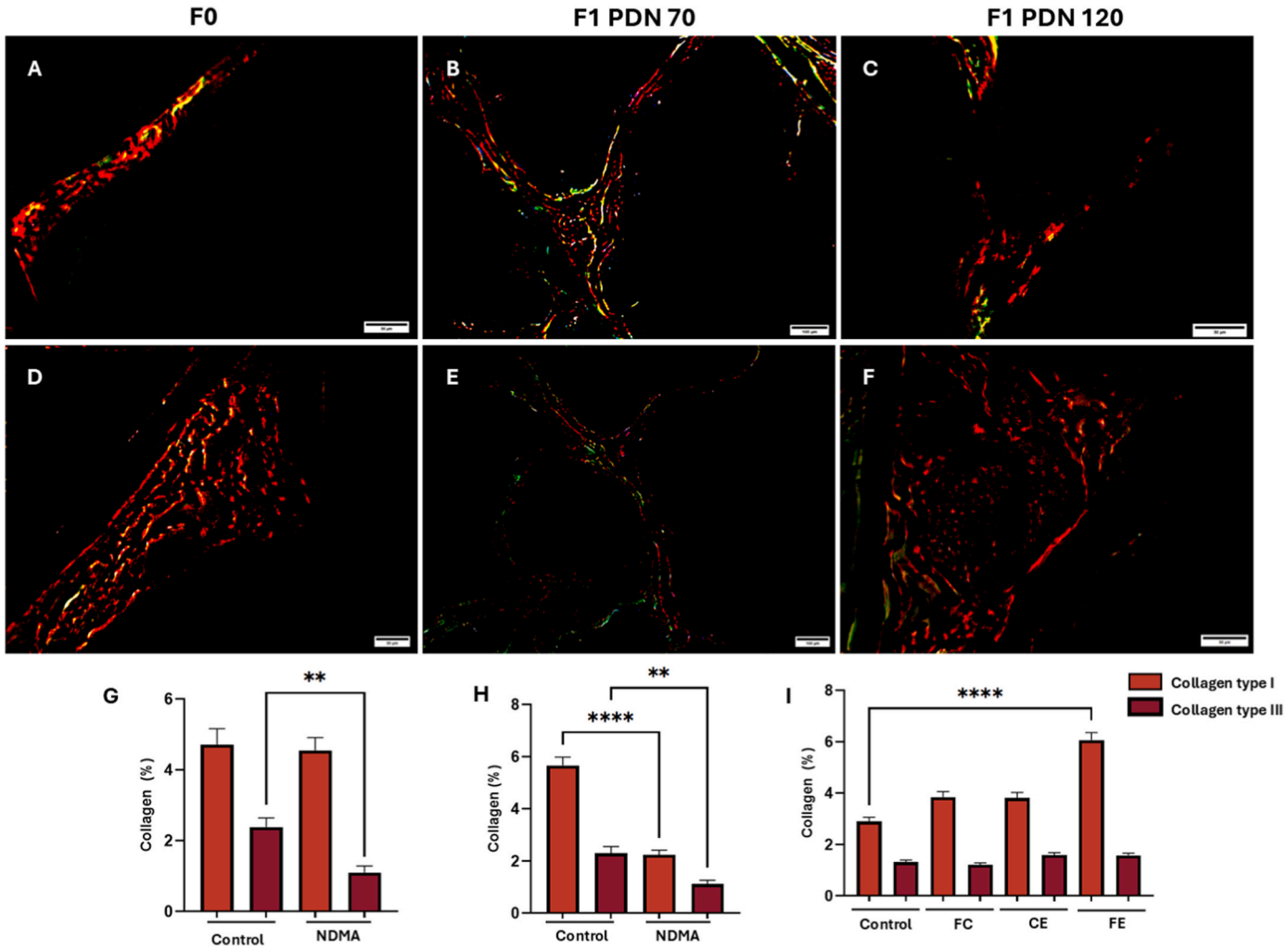

Fig. 2. Quantification of collagen type I and III. Polarized light visualization of F0 generation animals - Control (A) and exposed (C), F1 PND 70 - Control (B) and exposed (E), and F1 PND 120 – Control (C) and FE (F). Graphs represent the quantification of collagen type I and III of F0, F1 PND 70, and F1 PND 120 generations (G, H, and I) respectively (n = 5). Values expressed as median ± S.E.M. (n = 5 per group). Kruskall-Wallis post-test Dunn. **p < 0.01; ****p < 0.0001. PND. Postnatal day; FC, Exposed father and control offspring; CE, Control father and exposed offspring; FE, Exposed father and exposed offspring.

intact mast cells (Fig. 4G). A significant increase in degranulated mast cells was observed in all groups exposed to NDMA compared to control (Fig. 4H). There was no difference in the total number of mast cells in the prostate between the experimental groups (Fig. 4I). Histopathology images and mast cell count graphs are in Figs. 3 and 4 respectively.

The semi-quantitative histopathological analysis showed that, in the F0 generation, the NDMA group presented significantly higher inflammatory infiltrate scores compared with the control group (Fig. 3S), while no significant differences were observed between groups regarding the presence of cells in the glandular lumen (Fig. 3T).

In the F1 generation (PND120), inflammatory infiltrate scores were generally similar among the groups; however, the FE group showed significantly higher scores compared with the control group (Fig. 3U). For the presence of cells in the glandular lumen, no significant differences were observed among the experimental groups (Fig. 3V).

3.4. RT-qPCR

According to the results obtained by RT-qPCR, a significant reduction in *Ar* (androgen receptor) expression was observed exclusively in the F1 PND120 – FE group (Fig. 4I), when compared to control. Tumor necrosis factor-alpha (*Tnf-α*) gene expression showed a significant decrease in all F1 (PND120) generation groups exposed to NDMA (FC, CE, and FE) (Fig. 4J). Interleukin 6 (*Il-6*) expression significantly increased only in the F1 PND120 – FE group (Fig. 4K). No significant alteration in the Interleukin 10 (*Il-10*) expression were observed among the experimental groups.

3.5. Oxidative profile

3.5.1. Oxidative profile of the F0 generation

There was no significant change in lipid peroxidation, indicated by the concentration of thiobarbituric acid reactive substances (TBARS), in the F0 generation of the NDMA-exposed group compared to the control group (Fig. 5 A).

No significant changes were observed in glutathione-S-transferase activity (Fig. 5 B) and catalase (Fig. 5 C), nor in reduced glutathione concentration (Fig. 5 F). However, superoxide dismutase activity (Fig. 5 D) showed a significant increase in the NDMA-exposed group compared to the control group, and there was a reduction in total glutathione (Fig. 5 E) and oxidized glutathione (Fig. 5 G) concentrations.

4. Discussion

In this work, the exposure to NDMA in both paternal exposure and direct exposure during the sexual maturation of the F1 generation

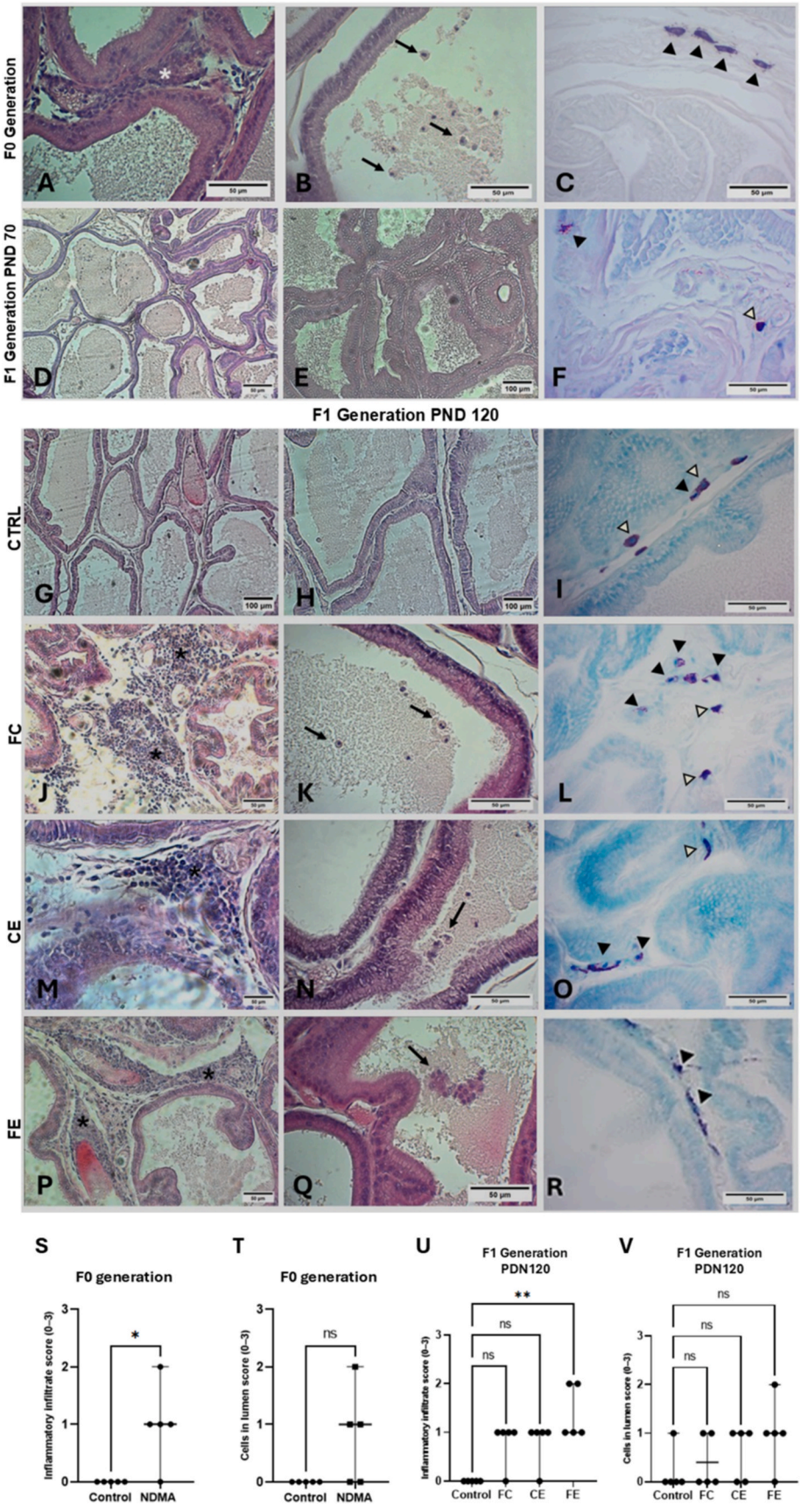

(caption on next page)

Fig. 3. Histopathology analysis. Photomicrograph of F0 generation - NDMA group (A-C). Photomicrograph of F1 PND 70 generation - control group (D) and NDMA group (E and F). Photomicrograph of F1 PND 120 generation - control group (G-H), FC (J-L), CE (M-O) and FE (P–R). D, G and H: normal morphology of the prostate. A, J, M and P: presence of inflammatory infiltrate in the interstitium (*). E, H and K: presence of cells in the lumen (arrow). B, K, N and Q. Degranulated mast cell (black arrowhead) and intact mast cell (white arrowhead). Semi-quantitative histopathological analysis is presented in (S–V): inflammatory infiltrate in F0 (S) and F1 PND120 (U), and presence of cells in the glandular lumen in F0 (T) and F1 PND120 (V). Staining in HE (A, B, D, E, G, H, J, K, K, M, N, P and Q); Staining with toluidine blue (C, F, I, L, O and R). PND. Postnatal day; FC, Exposed father and control offspring; CE, Control father and exposed offspring; FE, Exposed father and exposed offspring. Semi-quantitative histopathological scores (ordinal data). Mann–Whitney test was applied for comparisons between two groups (F0), and Kruskal–Wallis followed by Dunn's test was used for comparisons among four groups (F1). Data are presented as median and interquartile range (IQR). $P < 0.05$ was considered statistically significant. (For interpretation of the references to color in this figure legend, the reader is referred to the Web version of this article.)

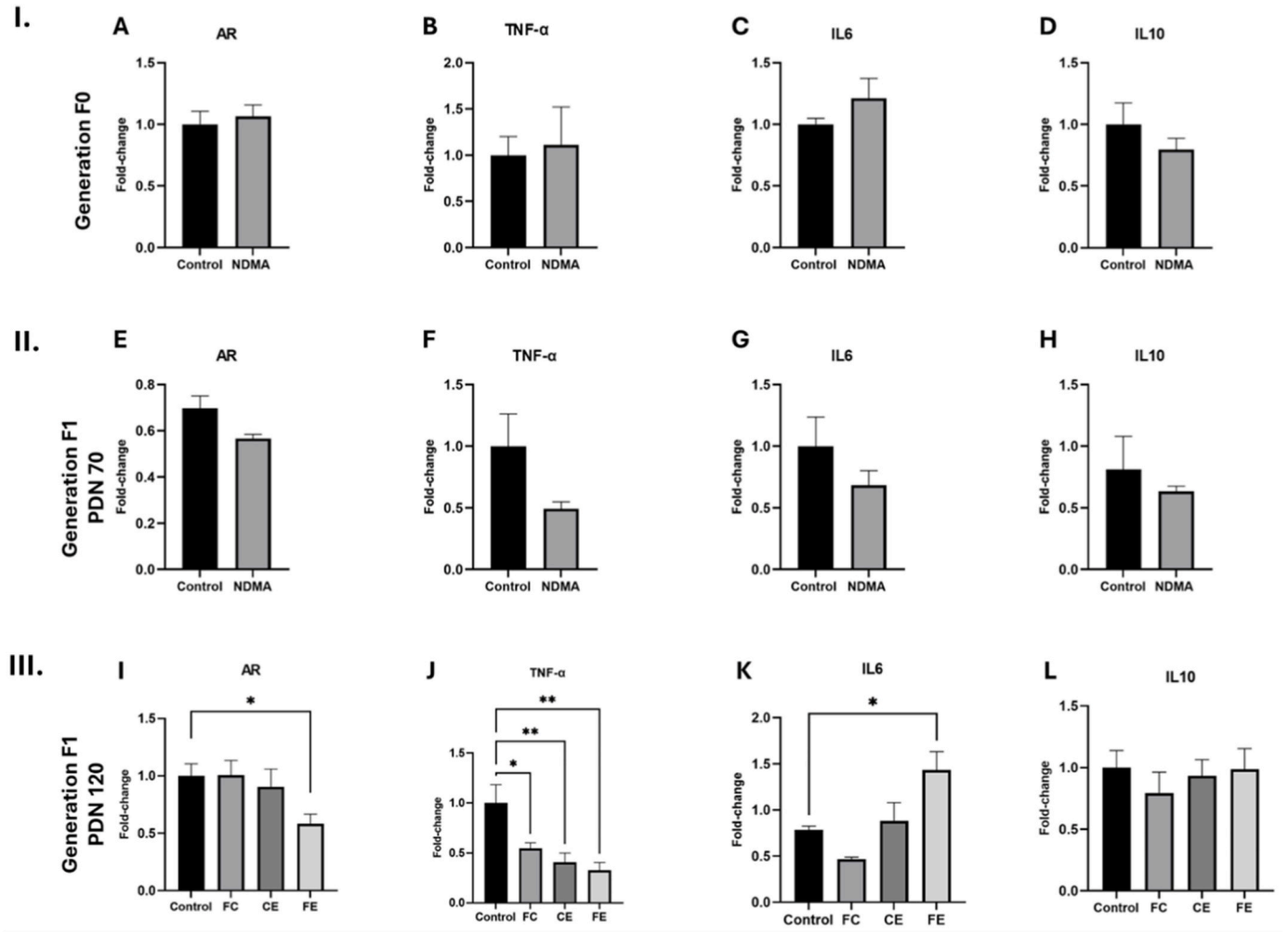

Fig. 4. Gene expression of Androgen Receptor (AR), Tumor Necrosis Factor-alpha (TNF-α), Interleukin 6 (IL6), and Interleukin 10 (IL10) in the prostate. (I) Generation F0 (PND 120); (II) Generation F1 (PND 70); (III) Generation F1 (PND 120). AR (A, E, I), TNF-α (B, F, J), IL6 (C, G, K), and IL10 (D, H, L). Values expressed as mean ± S.E.M. (n = 5 per group). Unpaired *t*-test. *p < 0.05; **p < 0.01 (Generation F0 and F1 PND 70). ANOVA test, with Dunnett's post hoc test. *p < 0.05; **p < 0.01 ***p < 0.001; ****p < 0.0001 (Generation F1 DPN 120). PND. Postnatal day; FC, exposed father and control offspring; CE, control father and exposed offspring; FE, father and exposed offspring.

altered the prostatic microenvironment, promoting immediate and persistent modifications that also manifested in adulthood. These effects were observed exclusively in the first filial generation (F1), characterizing intergenerational outcomes rather than transgenerational inheritance. These findings reinforce the concept of Paternal Origins of Health and Disease (POHaD), demonstrating that environmental factors transmitted by the father can durably impact the health of offspring and predispose them to prostatic alterations.

Glandular epithelial hyperplasia can occur as an adaptive response to degeneration and inflammation (Creasy et al., 2012), just as alterations in the prostatic epithelial compartment can reflect adaptive processes and/or lesions associated with NDMA-induced toxicity. Although there was no evident stereological alteration in the interstitium of the F0 generation, the reduction in collagen type III may reflect a modulation of collagen fibers, which is associated with remodeling processes in prostatic tissue (Tang, 2014).

According to Tang (2014), an imbalance between collagens types I and III can increase stiffness or compromise the elasticity of the prostatic stroma, favoring pathologies such as hyperplasia or cancer. In our study, the significant reduction in the interstitial compartment of the prostate was accompanied by a smaller area occupied by collagens type I and III in the F1 (PND70) generation after paternal NDMA exposure. These findings indicate that paternal exposure can modify the extracellular matrix constitution of the offspring, affecting both the quantity and proportion of collagens, and the concomitant reduction of collagens types I and III suggest a structural alteration of the stroma that may

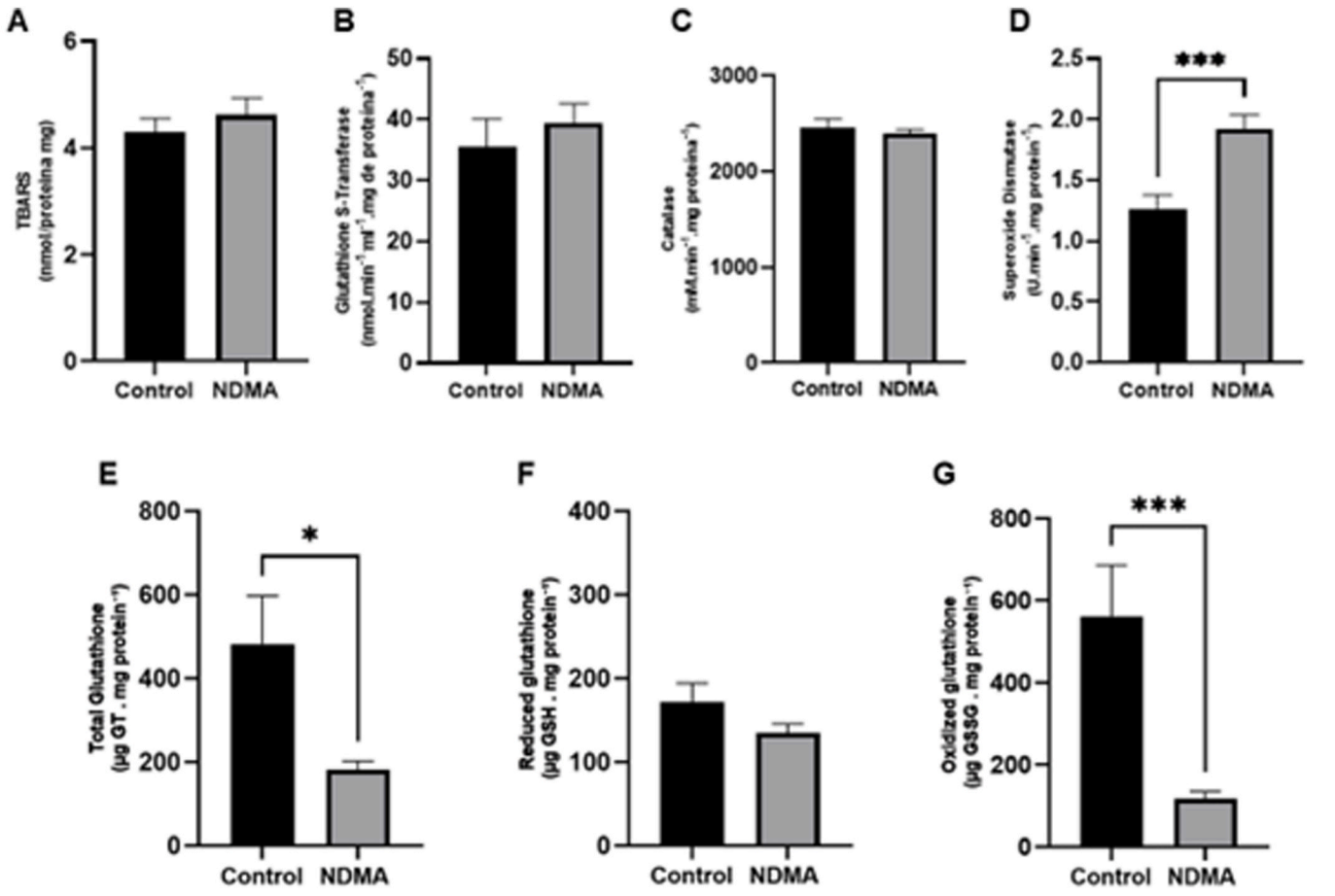

Fig. 5. Oxidative profile of the F0 generation. (A) Lipid peroxidation by concentration of thiobarbituric acid reactive substances (TBARS). (B) Glutathione-S-transferase activity. (C) Catalase activity. (D) Superoxide dismutase activity. (E) Total glutathione. (F) Reduced glutathione. (G) Oxidized glutathione. Data are expressed as mean ± S.E.M. (n = 10 per group). Unpaired *t*-test. ***p < 0,001.

compromise its support function. In contrast, in animals with combined exposure of father and offspring (FE), a significant increase in collagen type I was observed, demonstrating that the response to NDMA varies according to the experimental design. This increase may be related to fibrotic processes induced by NDMA toxicity, as prostatic fibrosis is frequently associated with active or chronic inflammation (Creasy; Bube; Rijk et al., 2012).

NDMA exposure has been associated with the induction of inflammatory processes through cellular mechanisms that favor the recruitment and activation of inflammatory cells (Adeleke & Adaramoye, 2021), as evidenced in the present study by the presence of inflammatory infiltrate in the prostatic interstitium and free cells in the lumen of the acini. Similar findings were described by Sheweita et al. (2017), who observed in adult rabbits after exposure to a single dose of 30 mg/kg/bw of NDMA via gavage, degeneration of testicular epithelial cells, accompanied by cellular detachment into the lumen of the seminiferous tubules. According to the authors, such alterations were attributed to the reduction of testosterone levels and the inhibition of the 17β-HSD enzyme, essential for the synthesis of this hormone.

Considering that the prostate is an androgen-dependent gland (Prins et al., 2001), and that hormonal disturbances can compromise the integrity of prostatic cellular junctions (Scarano et al., 2018), it is plausible that the cellular detachment observed in our results is also related to alterations in androgen signaling, given that the results of this study demonstrated a significant reduction in *Ar* gene expression, exclusively in the F1 generation FE group, where there was combined exposure to NDMA. Although the semi-quantitative histopathological analysis did not show statistically significant differences among the experimental groups, the observation of epithelial cells within the luminal compartment suggests subtle structural alterations that may not be fully captured by this scoring approach. AR is essential in maintaining prostatic homeostasis, regulating proliferation, epithelial differentiation, and glandular secretory activity (Heinlein; Chang, 2004). Thus, the decrease in the expression of this receptor can compromise androgenic function and contribute to the development of alterations in the prostate. The absence of this modulation in the other groups reinforces the hypothesis that combined exposure is necessary to trigger significant dysfunctions in the androgenic pathway.

In parallel, changes in inflammatory mediators were also observed in the F1 generation. The reduction in Tnf-α expression in all groups evaluated at PND120 (FC, CE, and FE) suggests a pattern of delayed immunological remodeling associated with NDMA, regardless of the exposure pathway. Furthermore, there was also an increase in *Il-6* expression exclusively in the FE group. Both TNF-α and IL-6 are important pro-inflammatory cytokines in regulating cell growth and death in the prostate (Wang et al., 2016). TNF-α can favor chronic inflammation and resistance to cell death by activating the NF-κB pathway (Chopra et al., 2004; Deichaite et al., 2022), while IL-6 stimulates proliferation, inhibits apoptosis, and contributes to a pro-inflammatory microenvironment that can favor prostatic lesions (Nguyen et al., 2014; Michalaki et al., 2004). The divergent regulation of these cytokines suggests a complex inflammatory milieu rather than a uniform pro- or anti-inflammatory state.

According to study by Desjardins et al. (1992), chronic low-dose oral

NDMA exposure (5 ppm and 10 ppm after 90 and 120 days) caused immunosuppression in young mice, affecting both humoral and cellular immune responses, even after exposure ceased. Although our results indicated a reduction in *Tnf-α* expression, this isolated finding does not support a state of immunosuppression. Given that there was also an increase in *Il-6* expression in the FE group and the presence of inflammatory infiltrate, the decrease in *Tnf-α* alone does not characterize an immunosuppression state, as it would require a predominance of immunosuppressive cells and/or loss of effective immune response, which was not observed (Goldmann et al., 2024). Thus, the data suggest that NDMA exposure induces delayed, low-grade chronic inflammation, contributing to remodeling of the prostatic microenvironment and reinforcing the concept of intergenerational immunomodulation.

The increase in mast cell degranulation in all experimental groups did not alter the recruitment of these cells in the prostatic tissue, except in the paternal exposure of the F1 generation (PND70), where there was a reduction in the total number of mast cells. As sentinel immune cells, mast cells regulate inflammatory processes, fibrosis, angiogenesis, and extracellular matrix remodeling through the release of mediators such as β-FGF, TGF-β, chymase, and tryptase (Beghdadi et al., 2011; Krystel--Whittemore et al., 2015; Trabucchi et al., 1998). Thus, the decreased number of intact mast cells indicates a state of persistent degranulation, potentially enhancing inflammatory activity and tissue remodeling processes within the prostate.

In the present study, the results of the oxidative profile of the F0 generation indicate that the reduction in GT and GSSG concentrations, associated with an increase in SOD activity after NDMA exposure, may have contributed to maintaining TBARS levels, indicating a possible protective effect against lipid peroxidation in prostatic cells.

The action of NDMA metabolites can elevate superoxide radical and hydrogen peroxide (H_2O_2) levels, potentially inducing an increase in oxidative stress (Adeleke; Adaramoye, 2016). Sheweita et al. (2017) observed in adult rabbits a reduction in the activity of these enzymes in the liver and testicles after a single dose of 30 mg/kg/bw of NDMA via gavage. Similarly, Adeleke and Adaramoye (2016) evidenced in young rats a decrease in the activity of antioxidant enzymes in the liver and kidney, including SOD, after exposure to 5 mg/kg/bw of NDMA intraperitoneally on two non-consecutive days. The observed discrepancy between the present study and previous research may be related to differences in the level of toxic exposure, cellular compensatory mechanisms, or even the dose-dependent response described by Calabrese and Baldwin (2001).

In the current study, exposure to a low dose of NDMA appears to have triggered an initial adaptive response, characterized by increased SOD activity, which indicates a protective mechanism to neutralize generated superoxide radicals. In contrast, higher doses of NDMA can overload the antioxidant system, leading to SOD dysfunction or depletion in other organs, as reported in other studies (Adeleke; Adaramoye, 2017; SHEWEITA et al., 2017). This information reinforces the importance of the balance between dose and response in NDMA toxicity, and that low-dose exposure causes changes in the antioxidant profile.

Regarding glutathiones, it is known that to prevent the accumulation of hydrogen peroxide (H2O2), glutathione peroxidase (GPx) acts by using GSH as an electron donor and converting it to GSSG (Ferreira; Matsubara, 1997). In our study, the reduction in GSSG levels in the NDMA-exposed group showed an attempt to maintain the redox balance of the prostate. Furthermore, this decrease in GSSG consequently affected the total glutathione (GT) concentration, which explains the reduction in GT concentration in the present study. Therefore, the antioxidant system is combating ROS generated by NDMA and preventing damage to the cell membrane, confirmed by unchanged TBARS levels.

Evidence suggests that paternal pre-gestational exposure to environmental factors can mediate intergenerational inheritance (Chen et al., 2016), and that adverse stimuli during critical developmental phases can result in prolonged alterations in organism structure and function (Lucas, 1991; Charmandari et al., 2005; Crews et al., 2007). In this context, it is highlighted that NDMA exposure, even at a low dose, can modulate the prostatic development of offspring from previously exposed fathers, reinforcing its intergenerational impact and the importance of future investigations, including germline and epigenetic endpoints.

In humans, exposure to NDMA typically occurs chronically at low levels through contaminated food, drinking water, and certain pharmaceutical products. This exposure is often intermittent and influenced by dietary habits, regional contamination levels, and regulatory controls. In contrast, the present study employed controlled daily oral administration to ensure consistent exposure and to isolate the biological effects of NDMA under defined experimental conditions. Although this design does not reproduce the variability of real-world human exposure patterns, it enables a mechanistic assessment of NDMA effects. Importantly, the dose used in this study falls within the range reported in contaminated consumable products, supporting the environmental and toxicological relevance of the findings while acknowledging the inherent limitations of the experimental model.

Finally, we highlight that this is the first study to evaluate prostatic parameters after direct and/or exclusively paternal exposure of rats to low-dose NDMA in two generations (F0 and F1), particularly during the preconception period and sexual maturation of the offspring. Future studies incorporating germline epigenetic analyses and additional generations are warranted to further elucidate the underlying mechanisms.

5. Conclusion

Our results indicate that the postnatal period represents a critical developmental window in which disturbances associated with paternal exposure can influence offspring development. Animals evaluated after direct postnatal exposure to NDMA also showed alterations, suggesting that both paternal programming and direct toxicological effects may contribute to the observed outcomes. Overall, the findings demonstrate that NDMA exposure can modulate gene expression and aspects of the prostatic microenvironment in the F1 generation. However, these results should be interpreted as intergenerational effects, and further studies are required to determine whether such alterations may persist in subsequent generations.

Declaration of generative AI and AI-assisted technologies in the manuscript preparation process

During the preparation of this work, the authors used *ChatGPT* (OpenAI) to revise grammar, clarity, and writing style, and *Adapta One* to translate the manuscript into English. After using these tools, the authors reviewed and edited the content as needed and take full responsibility for the content of the published article.

CRediT authorship contribution statement

Karen Gabriela Favaro de Souza: Writing – review & editing, Writing – original draft, Visualization, Validation, Methodology, Investigation, Formal analysis, Conceptualization. **Gabrielle Chalupa Faria:** Validation, Methodology, Formal analysis. **Débora Hipólito Quadreli:** Methodology, Investigation, Formal analysis. **Ivana Regina da Costa:** Methodology, Investigation, Formal analysis. **Bárbara Campos Jorge:** Investigation, Conceptualization. **Lívia Trippe Nagaoka:** Resources, Methodology, Data curation, Conceptualization. **Julia Stein:** Methodology, Investigation, Conceptualization. **Vanessa Aguiar Rocha:** Methodology, Formal analysis. **Arielle Cristina Arena:** Supervision, Funding acquisition, Conceptualization. **Wellerson Rodrigo Scarano:** Writing – review & editing, Supervision, Formal analysis. **Glaura Scantamburlo Alves Fernandes:** Writing – review & editing, Validation, Supervision, Resources, Methodology.

Declaration of competing interest

The authors declare that they have no known competing financial interests or personal relationships that could have appeared to influence the work reported in this paper.

Acknowledgments

The authors are grateful to CAPES (Coordinating Body for the Improvement of Postgraduate Studies in Higher Education) for providing a master scholarship to K. G. F. de Souza and partially financial support (Finance Code 001). This paper forms a part of the master's thesis of K. G. F. de Souza (State University of Londrina), supervised by G. S. A. Fernandes. We also express our gratitude to the National Council for Scientific and Technological Development (CNPq) for the Research Productivity Grant (PQ) No. 313704/2021-0, and São Paulo Research Foundation (FAPESP; Grant Nos. 2022/15364-7).

The authors thank the Centro Multiusuário de Laboratórios de Pesquisa (CMLP) of the Universidade Estadual de Londrina (UEL) for providing access to research equipment and technical assistance.

Appendix A. Supplementary data

Supplementary data to this article can be found online at https://doi.org/10.1016/j.fct.2026.116062.

Data availability

Data will be made available on request.

References

Adeleke, G.E., Adaramoye, O.A., 2016. Modulatory role of betulinic acid in N-nitrosodimethylamine-induced hepato-renal toxicity in male rats. Hum. Exp. Toxicol. 13, 1–10.

Adeleke, G.E., Adaramoye, O.A., 2017. Betulinic acid protects against N-nitrosodimethylamine-induced redox imbalance in testes of rats. Redox Rep. 22 (6), 556–562. https://doi.org/10.1080/13510002.2017.1322750.

Adeleke, G., Adaramoye, O., 2021. Betulinic acid abates N-nitrosodimethylamine-induced changes in lipid metabolism, oxidative stress, and inflammation in the liver and kidney of Wistar rats. J. Biochem. Mol. Toxicol. 35. https://doi.org/10.1002/jbt.22901.

Alves, J.T., Magalhães, L., Aquino, J. V. F. de, et al., 2025. Combined maternal and paternal low-dose N-nitrosodimethylamine exposure: maternal alterations and developmental toxicity in rats. Birth Defects Research 117 (10), e2540. https://doi.org/10.1002/bdr2.2540.

ANVISA, 2021. Guia sobre o Controle de Nitrosaminas em Insumos Farmacêuticos Ativos e Medicamentos. https://pesquisa.anvisa.gov.br/index.php/713856?lang=pt-BR.

Beard, J.C., Swager, T.M., 2021. An organic chemist's guide to *N*-Nitrosamines: their structure, reactivity, and role as contaminants. J. Org. Chem. 86 (3), 2037–2057. https://doi.org/10.1021/acs.joc.0c02774. Epub 2021 Jan 21. PMID: 33474939; PMCID: PMC7885798.

Beghdadi, W., et al., 2011. Mast cells as cellular sensors in inflammation and immunity. Front. Immunol. 2, 37. https://doi.org/10.3389/fimmu.2011.00037.

Calabrese, E.J., Baldwin, L.A., 2001. Hormesis: U-shaped dose responses and their centrality in toxicology. Trends Pharmacol. Sci. 22 (6), 285–291. https://doi.org/10.1016/S0165-6147(00)01719-3.

Carrara, I.M., et al., 2019. Looking beyond the skin: cutaneous and systemic oxidative stress in UVB-induced squamous cell carcinoma in hairless mice. J. Photochem. Photobiol. B Biol. 195, 17–26. https://doi.org/10.1016/J.JPHOTOBIOL.2019.04.007.

Charmandari, E., Tsigos, C., Chrousos, G., 2005. Endocrinology of the stress response. Annu. Rev. Physiol. 67, 259–284.

Chen, Q., et al., 2016. Sperm tsRNAs contribute to intergenerational inheritance of an acquired metabolic disorder. Science 351, 397–400.

Chen, Q., et al., 2017. Phthalate exposure, even below US EPA reference doses, was associated with semen quality and reproductive hormones: prospective MARHCS study in general population. Environ. Int. 104, 58–68. https://doi.org/10.1016/j.envint.2017.03.013.

Chopra, Dharam P., et al., 2004. TNF-α-mediated apoptosis in normal human prostate epithelial cells and tumor cell lines. Cancer Lett. 203 (2), 145–154. https://doi.org/10.1016/j.canlet.2003.09.016. Disponível em:

Creasy, D., Bube, A., Rijk, E. de, et al., 2012. Proliferative and nonproliferative lesions of the rat and mouse male reproductive system. Toxicol. Pathol. 40 (6_Suppl. l), 40S–121S. https://doi.org/10.1177/0192623312454337.

Crews, F., et al., 2007. Adolescent cortical development: a critical period of vulnerability for addiction. Pharmacol. Biochem. Behav. 86 (2), 189–199. https://doi.org/10.1016/j.pbb.2006.12.001.

Deichaite, I., et al., 2022. Differential regulation of TNFα and IL-6 expression contributes to immune evasion in prostate cancer. J. Transl. Med. 20 (1), 1–15.

Desjardins, R., Fournier, M., Denizeau, F., Krzystyniuk, K., 1992. Immunosuppression by chronic exposure to N-nitrosodimethylamine (NDMA) in mice. J. Toxicol. Environ. Health 37 (3), 351–361. https://doi.org/10.1080/15287399209531676.

Erthal, R.P., et al., 2017. Can resveratrol attenuate testicular damage in neonatal and adult rats exposed to 2,3,7,8-tetrachlorodibenzo-p-dioxin during gestation? Reprod. Fertil. Dev. https://doi.org/10.1071/RD17180.

FDA, 2020. FDA requests removal of all ranitidine products (Zantac) from the market. Disponível em: https://www.fda.gov/news-events/press-announcements/fda-requests-removal-all-ranitidine-products-zantac-market.

Ferreira, A.L.A., Matsubara, L.S., 1997. Radicais livres: conceitos, doenças relacionadas, sistema de defesa e estresse oxidativo. Rev. Assoc. Med. Bras. 43, 61–68.

Gibson-Corley, K.N., Olivier, A.K., Meyerholz, D.K., 2013. Principles for valid histopathologic scoring in research. Veterinary Pathology 50 (6), 1007–1015. https://doi.org/10.1177/0300985813485099. PubMed PMID: 23558974. PMCID: PMC3795863.

Goldmann, O., Nwofor, O.V., Chen, Q., Medina, E., 2024. Mechanisms underlying immunosuppression by regulatory cells. Front. Immunol. 15, 1328193. https://doi.org/10.3389/fimmu.2024.1328193. PMID: 38380317; PMCID: PMC10876998.

Golub, M.S., et al., 2008. Public health implications of altered puberty timing. Pediatrics 121, S218–S230.

Guerrero-Bosagna, C.M., Skinner, M.K., 2009. Epigenetic transgenerational effects of endocrine disruptors on male reproduction. Semin. Reprod. Med. 27 (5), 403–408. https://doi.org/10.1055/s-0029-1237428.

IMAGEJ, 2004. Image Processing and Analysis in Java. National Institutes of Health, Bethesda. https://imagej.nih.gov/ij/.

Kalinska, M., Meyer-Hoffert, U., Kantyka, T., Potempa, J. Kallikreins, 2016. The melting pot of activity and function. Biochimie 122, 270–282.

Keen, J.H., Habig, W.H., Jakoby, W.B., 1976. Mechanism for the several activities of the glutathione S-transferases. J. Biol. Chem. 251, 6183–6188. https://doi.org/10.1016/S0021-9258(20)81842-0.

Khoshkerdar, A., Eryasar, E., Morgan, H.L., Watkins, A.J., 2021. Impacts of paternal environment and lifestyle on maternal health during pregnancy. In: Reproduction, vol. 162. BioScientifica Ltd, pp. F101–F109. https://doi.org/10.1530/REP-20-0605, 5.

Krystel-Whittemore, M., Dileepan, K.N., Wood, J.G., 2015. Mast cell: a multifunctional master cell. Front. Immunol. 6, 620. https://doi.org/10.3389/fimmu.2015.00620.

Kumar, V.L., Majumder, P.K., 1995. Prostate gland: structure, functions and regulation. Int. Urol. Nephrol. 27 (3), 231–243. https://doi.org/10.1007/BF02564756.

Lee, H., Cho, M., 2024. The medical impact of the emerging ban on anti-hypertensive drugs contaminated with N-nitrosodimethylamine (NDMA): a nationwide longitudinal cohort study. J. Hypertens. 42 (Suppl. 1), e45–e46. https://doi.org/10.1097/01.hjh.0001019712.14943.9d.

Lucas, A., 1991. Programming by early nutrition in man. In: Bock, G.R., Whelan, J. (Eds.), The Childhood Environment and Adult Disease, CIBA Foundation Symposium 156. Wiley, Chichester, UK, pp. 38–55.

Mendes, L.O., et al., 2011. Mast cells and ethanol consumption: interactions in the prostate, epididymis and testis of UChB rats. Am. J. Reprod. Immunol. 66, 170–178. https://doi.org/10.1111/j.1600-0897.2010.00958.x.

Michalaki, V., Syrigos, K., Charles, P., Waxman, J., 2004. Serum levels of IL-6 and TNF-α correlate with clinicopathologic features and survival of prostate cancer patients. Br. J. Cancer 90 (12), 2312–2316.

Nash, J.P., Kime, D.E., Van Der Ven, L.T.M., Wester, P.W., Brion, F., Maack, G., Stahlschmidt-Allner, P., Tyler, C.R., 2004. Long-term exposure to environmental concentrations of the pharmaceutical ethynylestradiol causes reproductive failure in fish. Environ. Health Perspect. 112, 1725–1733.

Nguyen, D., Li, J., Tewari, A., 2014. Inflammation and prostate cancer: the role of interleukin 6 (IL-6). BJU Int. 6, 986–992.

Prins, G.S., et al., 2001. Influence of neonatal estrogens on rat prostate development. Reprod. Fertil. Dev. 13 (4), 241–252.

Punhagui, Paula Franco, et al., 2016. Ethanol exposure during peripubertal period increases the mast cell number and impairs meiotic and spermatic parameters in adult male rats. Microsc. Res. Tech. 79 (6), 541–549. https://doi.org/10.1002/jemt.22664.

Rahman, I., Kode, A., Biswas, S.K., 2007. Assay for quantitative determination of glutathione and glutathione disulfide levels using enzymatic recycling method. Nat. Protoc. 1, 3159–3165. https://doi.org/10.1038/nprot.2006.378.

Rocha, V.A., et al., 2023. 2, 4-dichlorophenoxyacetic acid (2, 4-D) exposure during postnataldevelopment alters the effects of western diet on mouse prostate. Reprod. Toxicol. 120, 108449.

Roth, T.L., Sweatt, J.D., 2011. Epigenetic marking of the Bdnf gene in the development and treatment of psychiatric disease. Nat. Neurosci. 14 (12), 1554–1556. https://doi.org/10.1038/nn.2975.

Russell, L.D., Ettlin, R.A., Sinha Hikim, A.P., Clegg, E.D., 1990. Histological and Histopathological Evaluation of the Testis. Clearwater, FL. Cache River Press.

Scarano, W.R., et al., 2009. Long-term effects of developmental exposure to di-n-butyl-phthalate (DBP) on rat prostate: proliferative and inflammatory disorders and a possible role of androgens. Toxicology 262 (3), 215–223.

Scarano, W.R., et al., 2018. Cell junctions in the prostate: an overview about the effects of endocrine disrupting chemicals (EDCS) in different experimental models. Reprod. Toxicol. 81, 147–154. https://doi.org/10.1016/j.reprotox.2018.08.009.

Senthilkumar, M., Amaresan, N., Sankaranarayanan, A., 2021. Plant-Microbe Interactions: Laboratory Techniques, vol. 1. Springer Science, Nova Iorque, pp. 117–118.

Sheweita, S.A., et al., 2017. N-nitrosamines induced infertility and hepatotoxicity in male rabbits. Environ. Toxicol. 32, 2212–2220. https://doi.org/10.1002/tox.22436.

Skinner, M.K., Anway, M.D., 2005. Seminiferous cord formation and germ-cell programming: epigenetic transgenerational actions of endocrine disruptors. Ann. N. Y. Acad. Sci. 1061, 18–32.

Soubry, Adelheid, et al., 2014. A paternal environmental legacy: evidence for epigenetic inheritance through the male germ line. Bioessays 36 (4), 359–371.

Sugimura, Y., Cunha, G.R., Donjacour, A.A., 1986. Morphogenesis of ductal networks in the mouse prostate. Biol. Reprod. 34 (5), 961–971.

Tang, J., et al., 2014. Tissue elasticity demonstrated by elastography and its correlation with type I and type III collagen characteristics in prostatic stroma. Asian J. Androl. 16 (2), 305–308. https://doi.org/10.4103/1008-682X.122582.

Trabucchi, E., Radaelli, E., Marazzi, M., Foschi, D., Musazzi, M., Veronesi, A.M., Montorsi, W., 1998. The role of mast cells in wound healing. Int J Tecido Reagir 10, 367–372.

UNITED STATES ENVIRONMENTAL PROTECTION AGENCY (EPA), 2014. Technical fact sheet – NDMA. https://nepis.epa.gov/Exe/ZyPURL.cgi?Dockey=P100LTGG.TXT.

US-EPA, 2016. Six-Year Review 3 Technical Support Document for Nitrosamines.

Wang, L., et al., 2016. Expression of IL-6 and TNF-α in Benign Prostatic Hyperplasia Combined with Histological Inflammation.

Wilson, J., 2011. The critical role of androgens in prostate development. Endocrinol Metab. Clin. N. Am. 40 (3), 577–590. https://doi.org/10.1016/j.ecl.2011.05.003.

Zhang, C., Bruins, M.E., Yang, Z., Liu, S., Rao, P., 2016. A new formula to calculate activity of superoxide dismutase in indirect essays. Anal. Biochem. 503, 65–67.